Model Reconstruction for Moment-based Stochastic Chemical Kinetics

Alexander Andreychenko, Saarland University
Linar Mikeev, Saarland University
Verena Wolf, Saarland University

Based on the theory of stochastic chemical kinetics, the inherent randomness and stochasticity of biochemical reaction networks can be accurately described by discrete-state continuous-time Markov chains. The analysis of such processes is, however, computationally expensive and sophisticated numerical methods are required. Here, we propose an analysis framework in which we integrate a number of moments of the process instead of the state probabilities. This results in a very efficient simulation of the time evolution of the process. In order to regain the state probabilities from the moment representation, we combine the fast moment-based simulation with a maximum entropy approach for the reconstruction of the underlying probability distribution. We investigate the usefulness of this combined approach in the setting of stochastic chemical kinetics and present numerical results for three reaction networks showing its efficiency and accuracy. Besides a simple dimerization system, we study a bistable switch system and a multi-attractor network with complex dynamics.

1. INTRODUCTION

During the last two decades discrete stochastic models have become a very popular description of biochemical reactions that take place in living organisms. They provide an appropriate representation of the discrete molecular populations in the cell and accurately mimic the inherent randomness and discreteness of molecular interactions [Fedoroff and Fontana 2002; McAdams and Arkin 1999; Thattai and van Oudenaarden A. 2001; Elowitz et al. 2002].

The theory of stochastic chemical kinetics gives a rigorously justified stochastic description in terms of discrete-state continuous-time Markov chains [Gillespie 1977]. The dynamics of the chain is governed by the Chemical Master Equation (CME) which describes the time evolution of the state probabilities. However, the CME can be solved

analytically only in a very limited number of cases. The main difficulty arising in the numerical solution of the CME is the curse of dimensionality: each chemical species that is involved in a reaction adds one dimension to the state space of the Markov chain since the state of the chain is given by a population vector counting the current number of molecules for each species. Tight bounds for molecular counts are usually not known a priori and thus the size of the state space that has to be considered is extremely large or even infinite rendering the direct numerical integration of the CME infeasible. Sophisticated truncation approaches have been developed [Munsky and Khammash 2006; Mateescu et al. 2010a; Andreychenko et al. 2012] which work well as long as the average population sizes remain small. The main idea is to concentrate on those population vectors containing a significant amount of probability mass. In this way only very rare behavior of the process is neglected. If the reaction network contains highly abundant chemical species then the underlying probability distribution of the process becomes very large, even when insignificant parts are truncated. In such a case it is advantageous to change the representation of the distribution. The idea of methods of moments or moment closure methods is to replace the distribution of the Markov chain by its moments up to a certain finite order [Engblom 2006; Ale et al. 2013]. It is possible to derive differential equations that can be used to approximate the time evolution of the moments. For instance, if the distribution of the chain is similar to a multivariate normal distribution, one can obtain a very accurate approximation of the distribution by tracking the average molecule counts and their variances and covariances over time. For systems exhibiting more complex behavior such as oscillations or multi-modality, moments of higher order are necessary for an accurate description [Ale et al. 2013]. For instance, the moments of order three typically describe the skewness of the distribution while moments of order four are known to be a measure of the width of the tails of the distribution.

Often one is interested in the probability of certain events or in likelihoods of observations of the process. However, usually prior information regarding the properties of the distribution (e.g. approximately normally distributed) is not given and in such a case regaining the probability distribution from the moment description is non-trivial. In fact it turns out that this problem, known as the classical moment problem, has a long history in other application domains and only recently very efficient methods for the reconstruction of the distribution became available.

Given a number of moments of a random variable, there is in general no unique solution for the corresponding distribution. However it is possible to define a sequence of distributions that converges to the true one whenever the number of constraints approaches infinity [Mnatsakanov and Hakobyan 2009]. Conditions for the existence of a solution are well-elaborated (such as Krein's and Carlemann's conditions) but they do not provide a direct algorithmic way to create the reconstruction. Therefore, Pade approximation [Mead and Papanicolaou 1984] and inverse Laplace transform [Chauveau et al. 1994] have been considered but turned out to work only in restricted cases and require a large number of constraints. Similar difficulties are encountered when lower and upper bounds for the probability distribution are derived [Gavriliadis 2008; Tari et al. 2005; Kaas and Goovaerts 1986]. Kernel-based approximation methods have been proposed where one restricts to a particular class of distributions [Gavriliadis and Athanassoulis 2012; Mnatsakanov and Hakobyan 2009; Chen 2000]. The numerically most stable methods are, however, based on the maximum entropy principle which has its roots in statistical mechanics and information theory. The idea is to choose from all distributions that fulfill the moment constraints the distribution that maximizes the entropy. The maximum entropy reconstruction is the least biased estimate that fulfills the moment constraints and it makes no assumptions about the missing information. No additional knowledge about the shape of the distribution neither a large number of

moments is necessary. For instance, if only the first moment (mean) is provided the result of applying the maximum entropy principle is exponential distribution. In case of two moments (mean and variance) the reconstruction is given by normal distribution. Additionally, if experimental data (or simulation traces) is available, data-driven maximum entropy methods can be applied [Wu 2009; Amos et al. 1996]. Recently, notable progress has been made in the development of numerical methods for the moment constrained maximum entropy problem [Abramov 2010; Bandyopadhyay et al. 2005; Mead and Papanicolaou 1984], where the main effort is put to the transformation of the problem in order to overcome the numerical difficulties that arise during the optimization procedure.

In this paper we propose a combination of the maximum entropy reconstruction and the moment closure approach for the solution of the CME. We approximate the moments over time and for a particular time instant of interest we reconstruct the underlying distribution with a moment constrained maximum entropy approach. We do not make any further assumptions about the distribution and study the feasibility, efficiency and accuracy of this combined approach. To the best of our knowledge, the maximum entropy approach has not yet been applied to stochastic models of biochemical reaction networks before. We consider three example networks which are small enough such that we can compare our results with a nearly exact solution obtained via a direct numerical integration of the CME. The maximum entropy approach has been applied to chemical reaction networks in [Smadbeck and Kaznessis 2013]. However, they restrict to finite-state models where the entropy maximization becomes much easier since the support of the distribution is bounded. Here, we allow for infinite state space and present two infinite-state case studies. In addition, Smadbeck and Kaznessis compare their results with statistical estimates obtained from Monte-Carlo simulations while we compare to results obtained via a numerical solution for which the approximation error is known. Two of the examples that we consider have multi-modal distributions which makes the reconstruction harder. However, our findings show that the combination of moment closure and maximum entropy reconstruction is surprisingly accurate also for complex systems and it is very efficient in terms of running times. In particular, the reconstruction part is very fast so that the main advantage of the moment closure method - the short running time - remains, even if it is combined with the maximum entropy approach. Thus, it provides a very useful alternative to other analysis methods such as Monte Carlo simulations of the CME. In particular, most methods do not scale in the number of molecules while the efficiency of the moment closure approach is independent of the population sizes. Short running times are particularly important if parameters of the process have to be adjusted or if experiments must be designed [Ruess et al. 2013], since for such problems the model has to be analyzed for many different parameter combinations.

The paper is further organized as follows: we introduce our model in Section 2 and shortly explain how the CME can be numerically integrated to obtain accurate results for small systems. In Section 3 we discuss how the moment closure approach is applied to the CME and in Section 4 we describe the details of the maximum entropy approach and how it can be used to reconstruct the distribution from a number of moments. Finally, we present experimental results for the three case studies in Section 5 and conclude the paper with Section 6.

2. STOCHASTIC CHEMICAL KINETICS

Stochastic chemical kinetics refers to a widely-used modelling framework for the description of networks of biochemical reactions [McQuarrie 1967]. We consider a biological compartment (e.g. a living cell) in which molecules of different types undergo chemical reactions. Assuming that this reaction volume is well-stirred and in

thermal equilibrium, it is possible to physically justify a Markov chain description of the chemical populations [Gillespie 1977], that is, we consider a random vector $X(t) = (X_1(t), \ldots, X_n(t))$ where $X_i(t)$ is the number of molecules of type i at time t ($i \in \{1, \ldots, n\}, t \geq 0$). We assume that the set of possible reactions is given by the stoichiometric equations

$$R_j : \qquad \ell_{j,1} S_1 + \ldots + \ell_{j,n} S_n \xrightarrow{c_j} \tilde{\ell}_{j,1} S_1 + \ldots + \tilde{\ell}_{j,n} S_n, \quad 1 \leq j \leq m.$$
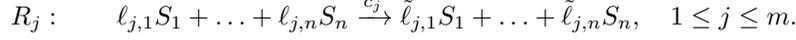
Here, $\ell_{j,i}$ and $\tilde{\ell}_{j,i}$ refer to the number of molecules used up and produced by the reaction, respectively ($\ell_{j,i}, \tilde{\ell}_{j,i} \in \mathbb{N}_0$ and $1 \leq i \leq m$) and c_j is the so-called stochastic reaction rate constant that determines the probability of the reaction as explained in the sequel.

EXAMPLE 1. *We consider a simple dimerization example [Ale et al. 2013] with the stoichiometric equations*

$$\begin{aligned} R_1 : & \quad 2P \xrightarrow{c_1} P_2, \\ R_2 : & \quad P_2 \xrightarrow{c_2} 2P, \end{aligned}$$

(1)

where $\ell_{1,1} = \tilde{\ell}_{2,1} = 2$, $\ell_{2,2} = \tilde{\ell}_{1,2} = 1$ and $\ell_{1,2} = \ell_{2,1} = \tilde{\ell}_{1,1} = \tilde{\ell}_{2,2} = 0$. Note that we omit terms which are zero and the factors equal to one.

2.1. Transition Rates

Let $v_j \in \mathbb{Z}^n$ be the vector that describes the population change of reaction R_j, that is, $v_j = (\tilde{\ell}_{j,1} - \ell_{j,1}, \ldots, \tilde{\ell}_{j,n} - \ell_{j,n})$. Transitions of the Markov chain X correspond to chemical reactions and the transition rate of reaction R_j is given by

$$\lim_{h \to 0} \frac{1}{h} P(X(t+h) = x + v_j \mid X(t) = x) = c_j \prod_{i=1}^{n} \binom{x_i}{\ell_{j,i}}$$

where $x = (x_1, \ldots, x_n) \in \mathbb{N}_0^n$ is a state and the binomial coefficients describe the number of possible combinations of reactant molecules. Note that c_j depends on the physical properties of the reactants as well as on the temperature and the size of the reaction volume. Here we make the usual assumption that c_j is constant in time. It is possible to extend the results presented in the sequel for time-dependent c_j. In this case the underlying Markov chain is time-inhomogeneous and an accurate simulation may be challenging if the rates strongly vary in time [Andreychenko et al. 2011].

In the sequel we also restrict to chemical reactions that are at most bimolecular, i.e., we assume that $\sum_{i=1}^{n} \ell_{j,i} \in \{0, 1, 2\}$, which is a reasonable assumption because reactions where more than two molecules have to collide can usually be decomposed into smaller ones where at most two molecules have to collide [Gillespie 1977].

2.2. Chemical Master Equation

The dynamics of X is given by the chemical master equation that describes the time evolution of the transient distribution $\pi(x, t) = P(X(t) = x)$ as a linear ordinary differential equation

$$\frac{\partial \pi(x, t)}{\partial t} = \sum_{j=1}^{m} \left(\alpha_j(x - v_j) \pi(x - v_j, t) - \alpha_j(x) \pi(x, t) \right). \tag{2}$$

Here, $\alpha_j(x) = c_j \prod_{i=1}^{n} \binom{x_i}{\ell_{j,i}}$ is the transition rate in state x for reaction R_j. If an initial distribution, say at time $t = 0$, is given then the equation has a unique solution at all

finite times $t \geq 0$. It is important to note that often the number of states with $\pi(x, t) > 0$ is infinite since bounds on the population sizes are not known a priori. Thus, although in reality the molecule numbers are always finite, theoretically an infinite number of states can have positive probability. This leads to two complications compared to finite-state models. First, the limiting distribution of the Markov chain may not exist and additional conditions are necessary to ensure the existence [Dayar et al. 2011]. And second, truncation techniques are necessary to numerically simulate (2) since only a tractable number of states can be considered in each integration step. Only in special cases an analytic solution of (2) is available [Jahnke and Huisinga 2007].

2.3. Direct Numerical Simulation

In the sequel we shortly explain how the master equation in (2) can be simulated numerically since our goal is to compare a moment closure approximation combined with a reconstruction of the individual probabilities with such a direct numerical simulation. The latter performs well as long as the average population sizes remain small and the approximation error can be controlled by a simple threshold criterion. Thus, we will be able to determine the accuracy of the moment closure approximation as well as the accuracy of the reconstruction algorithm.

The direct numerical simulation that we consider is based on the dynamic state space truncation developed for uniformization methods [Mateescu et al. 2010b] and for integration schemes such as Runge Kutta methods [Andreychenko et al. 2012; Mikeev et al. 2011]. The main idea is to exploit the inflow-outflow form of (2) for the construction of the dynamic state space. The terms $\alpha_j(x - v_j)\pi(x - v_j, t)$ can be seen as the inflow to state x for reaction R_j while $\alpha_j(x, t)\pi(x, t)$ is the corresponding outflow. Let $p(x, t)$ be the approximation of $\pi(x, t)$ during the numerical integration for all x and all $t \geq 0$. Initially we set $p(x, 0) = \pi(x, 0)$ and during an integration step for the interval $[t, t + h)$ we start with a subset $S^{(t)}$ of states that have significant probability at time t, i.e.,

$$S^{(t)} := \{x \mid p(x, t) > \delta_1\}$$

where $\delta_1 > 0$ is a small threshold. For all states not in $S^{(t)}$ we let $p(x, t) = 0$. During the numerical integration we add new states to $S^{(t)}$ whenever they receive a significant amount of inflow, i.e. if we use the explicit Euler method, the new state probability at time $t + h$ is calculated as

$$p(x, t + h) = p(x, t) + h \cdot \sum_{j=1}^{m} \left(\alpha_j(x - v_j)p(x - v_j, t) - \alpha_j(x)p(x, t) \right).$$

For a state $x \notin S^{(t)}$ this reduces to

$$p(x, t + h) = h \cdot \sum_{j=1}^{m} \alpha_j(x - v_j)p(x - v_j, t).$$

Hence, we can loop over all states in $S^{(t)}$ and, before integrating their probability, check whether their successors receive significant inflow. More precisely, we simply add a state x to the set $S^{(t)}$ if $h \cdot \alpha_j(x - v_j)p(x - v_j, t) > \delta_2$ for some j. Here, δ_2 is again a small threshold. We then also compute $p(x, t + h)$ for this new state. It turns out that for most example networks an accurate approximation is obtained if we work with a single threshold $\delta_1 = \delta_2 =: \delta$ and choose $\delta \in \{10^{-10}, 10^{-9} \ldots, 10^{-5}\}$. Note that the new set $S^{(t+h)}$ will then contain all states $x \in S^{(t)}$ whose probability at time $t + h$ is at least δ as well as all successors $x + v_j \notin S^{(t)}$ where $x \in S^{(t)}$ and there exists a j such that $h \cdot \alpha_j(x - v_j)p(x - v_j, t) > \delta$ (which implies that their probability at time $t + h$ is at least
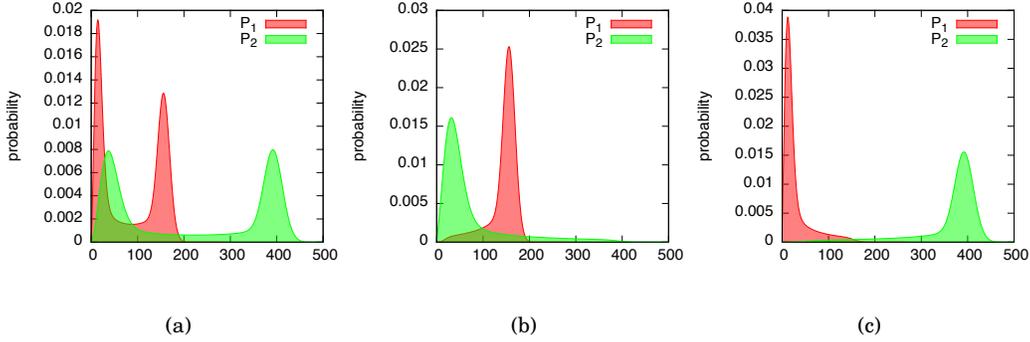
Fig. 1: Probability distribution of the protein counts P_1 and P_2 conditioned on the events that the promotor region is (a) free (b) bound to P_1, and (c) bound to P_2, computed at time instant $t = 100$ for exclusive switch system.

δ). Obviously, different truncation strategies are possible (e.g. choose δ_2 smaller than δ_1). However, we found that simply adding all successors ($\delta_2 = 0$) is not efficient since often we have reversible reactions, i.e., $v_j = -v_k$ for some $j \neq k$ where one direction is much more likely then the other, say R_j. In such a case the main part of the probability mass moves in the direction of v_j and the accuracy gain in adding a successor w.r.t. v_k is not worth the effort since during the next construction of $S^{(t)}$ these successors are anyway removed from $S^{(t)}$.

In order to illustrate the method, we list the size of the truncated state space and the total loss of probability mass for the following example:

EXAMPLE 2. *We consider a gene regulatory network called the exclusive switch [Loinger et al. 2007]. It describes the dynamics of two genes with an overlapping promotor region, and their products P_1 and P_2. Molecules of both species P_1 and P_2 are produced if no transcription factor is bound to the promotor region (region is free). However if a molecule of type P_1 (P_2) is bound to the promotor then it inhibits the expression of the other product, i.e. only molecules of P_2 (P_1) can be produced. Only one molecule can be bound to the promotor region at a time. The model has an infinite state space and the stoichiometric equations are given by:*

$$DNA \xrightarrow{c_1} DNA + P_1 \qquad DNA + P_1 \xrightarrow{c_5} DNA.P_1$$

$$DNA \xrightarrow{c_2} DNA + P_2 \qquad DNA + P_2 \xrightarrow{c_6} DNA.P_2 \qquad DNA.P_1 \xrightarrow{c_9} DNA.P_1 + P_1$$

$$P_1 \xrightarrow{c_3} \emptyset \qquad\qquad DNA.P_1 \xrightarrow{c_7} DNA + P_1 \qquad DNA.P_2 \xrightarrow{c_{10}} DNA.P_2 + P_2$$

$$P_2 \xrightarrow{c_4} \emptyset \qquad\qquad DNA.P_2 \xrightarrow{c_8} DNA + P_2$$
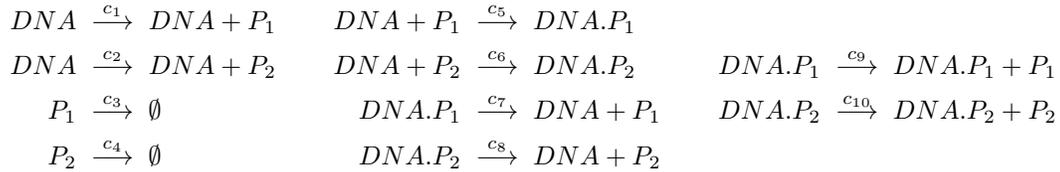
where the reaction rate constants $c_1, \ldots, c_{10}$ are given by the entries of the vector $c = (2.0, 5.0, 0.005, 0.005, 0.005, 0.002, 0.02, 0.02, 2.0, 5.0)$ and the initial conditions are such that only one DNA molecule is present in the system while the molecular counts for the rest of species are zero.

In Figure 1 we plot the results of a direct numerical simulation using the dynamical state space as explained above. The different subfigures show the marginal distributions of protein counts P_1 and P_2 when we condition on the three different states of the promotor region (free, P_1 or P_2 bound). To investigate the accuracy of the obtained re-

sults we refer to the Table I, where we list the amount ϵ of probability mass lost during the computation and the size $|S|$ of the truncated state space $S^{(t)}$ for different thresholds δ at time instant $t = 100$. Note that the probability of all states not in $S^{(t)}$ is approximated as zero. Thus, ϵ is equal to the total approximation error (sum of all state-wise errors) and all computed state probabilities are underapproximations, i.e.

$$\sum_x \pi(x,t) - \sum_x p(x,t) \leq \epsilon \tag{3}$$

where we have equality at the final time instant of the computation. We find that, for instance, if we choose $\delta = 10^{-15}$ the total approximation error remains below 10^{-10}.

3. MOMENT CLOSURE APPROXIMATION

As opposed to the method in the previous section, during the moment closure approximation we integrate the first k moments of the distribution $\pi(x,t)$ over time. For this we derive a system of differential equations for the moments along the lines of Ale et al. to show how and where approximations errors occur [Ale et al. 2013]. We restrict ourselves to the first two moments in order to keep this review of moment closure techniques short and also because the derivation of the equations for the first two moments are sufficient for illustrating the technique.

Let $f : \mathbb{N}_0^n \to \mathbb{R}^n$ be a function that is independent of t. In the sequel we will exploit the relationship

$$
\begin{aligned}
\tfrac{d}{dt} E\left(f(X(t))\right) &= \sum_x f(x) \cdot \tfrac{d}{dt} P(X(t) = x) \\
&= \sum_{j=1}^m E\left(\alpha_j(X(t)) \cdot \left(f(X(t) + v_j) - f(X(t))\right)\right).
\end{aligned}
\tag{4}
$$

For $f(x) = x$ this yields a system of equations for the population means

$$\tfrac{d}{dt} E\left(X(t)\right) = \sum_{j=1}^m v_j E\left(\alpha_j(X(t))\right). \tag{5}$$

Note that for bimolecular reactions, $E\left(\alpha_j(X(t))\right)$ is equal to

$$
\begin{aligned}
&c_j E\left(X_i(t) \cdot X_{i'}(t)\right) \neq c_j E\left(X_i(t)\right) \cdot E\left(X_{i'}(t)\right) &&\text{if } i \neq i', \\
&0.5 c_j E\left(X_i(t) \cdot (X_{i'}(t) - 1)\right) \neq 0.5 c_j E\left(X_i(t)\right) \cdot \left(E\left(X_{i'}(t)\right) - 1\right) &&\text{if } i = i',
\end{aligned}
$$

for $i, i' \in \{1, \ldots, n\}$, which means that the system of ODEs in Eq. (5) is only closed if at most monomolecular reactions ($\sum_{i=1}^n \ell_{j,i} \leq 1$) are involved. For most networks the latter condition is not true but we can approximate the unknown term $E\left(X_i(t) \cdot X_{i'}(t)\right)$ either by assuming that the covariance is zero, which gives $E\left(X_i(t) \cdot X_{i'}(t)\right) = E\left(X_i(t)\right) \cdot E\left(X_{i'}(t)\right)$ or by extending the system in (5) with additional equations for the second moments. The general strategy is to replace $\alpha_j(X(t))$ by a Taylor series about the mean $E\left(X(t)\right)$. Let us write $\mu_i(t)$ for $E\left(X_i(t)\right)$ and $\mu(t)$ for the vector with entries $\mu_i(t)$,

Table I: Dynamical state space truncation results for the exclusive switch

δ	$|S|$	ϵ	time (sec)
10^{-10}	183210	$3 \cdot 10^{-6}$	154
10^{-12}	203948	$2 \cdot 10^{-8}$	174
10^{-15}	265497	$9 \cdot 10^{-11}$	239
10^{-20}	381374	$1 \cdot 10^{-13}$	1027

$1 \leq i \leq n$. Then

$$E\left(\alpha_j(X)\right) \;=\; \alpha_j(\mu) + \tfrac{1}{1!}\sum_{i=1}^{n} E\left(X_i - \mu_i\right)\tfrac{\partial}{\partial x_i}\alpha_j(\mu)$$
$$+ \tfrac{1}{2!}\sum_{i=1}^{n}\sum_{k=1}^{n} E\left((X_i - \mu_i)(X_k - \mu_k)\right)\tfrac{\partial^2}{\partial x_i \partial x_k}\alpha_j(\mu) + \ldots$$

where we omitted t in the equation to improve the readability. Note that $E\left(X_i(t) - \mu_i\right) = 0$ and since we restrict to reactions that are at most bimolecular, all terms of order three and more disappear. By letting C_{ik} be the covariance $E\left((X_i(t) - \mu_i)(X_k(t) - \mu_k)\right)$ we get

$$E\left(\alpha_j(X)\right) \;=\; \alpha_j(\mu) + \tfrac{1}{2}\sum_{i=1}^{n}\sum_{k=1}^{n} C_{ik}\tfrac{\partial^2}{\partial x_i \partial x_k}\alpha_j(\mu) \tag{6}$$

Next, we derive an equation for the covariances by first exploiting the relationship

$$\tfrac{d}{dt}C_{ik} = \tfrac{d}{dt}E\left(X_i X_k\right) - \tfrac{d}{dt}(\mu_i \mu_k) = \tfrac{d}{dt}E\left(X_i X_k\right) - (\tfrac{d}{dt}\mu_i)\mu_k - \mu_i(\tfrac{d}{dt}\mu_k) \tag{7}$$

and if we couple this equation with the equations for the means, the only unknown term that remains is the derivative $\tfrac{d}{dt}E\left(X_i X_k\right)$ of the second moment. For this we can use the same strategy as before, i.e., from Eq. (4) we get

$$\tfrac{d}{dt}E\left(X_i X_k\right) = \sum_{j=1}^{m}\left[v_{j,i}v_{j,k}E\left(\alpha_j(X)\right) + v_{j,k}E\left(\alpha_j(X)X_i\right) + v_{j,i}E\left(\alpha_j(X)X_k\right)\right] \tag{8}$$

where $v_{j,i}$ and $v_{j,k}$ are the corresponding entries of the vector v_j. Clearly, we can use Eq. (6) for the term $E\left(\alpha_j(X)\right)$ while the terms $E\left(\alpha_j(X)X_i\right)$ and $E\left(\alpha_j(X)X_k\right)$ have to be replaced by the corresponding Taylor series about the mean. Let $f_j(x) := \alpha_j(x)x_i$. Similar to Eq. (6) we get

$$E\left(\alpha_j(X)X_i\right) \;=\; \alpha_j(\mu)\mu_i + \tfrac{1}{1!}\sum_{i=1}^{n} E\left(X_i - \mu_i\right)\tfrac{\partial}{\partial x_i}f_j(\mu)$$
$$+ \tfrac{1}{2!}\sum_{i=1}^{n}\sum_{k=1}^{n} E\left((X_i - \mu_i)(X_k - \mu_k)\right)\tfrac{\partial^2}{\partial x_i \partial x_k}f_j(\mu) + \ldots. \tag{9}$$

Here, it is important to note that moments of order three come into play since derivatives of order three of $f_j(x) = \alpha_j(x)x_i$ may be nonzero. It is possible to take these terms into account by deriving additional equations for moments of order three and higher. Obviously, these equations will then include moments of even higher order such that theoretically we end up with an infinite system of equations. However, a popular strategy is to close the equations by assuming that all moments of order $> M$ that are centred around the mean are equal to zero. E.g. if we choose $M = 2$, then we can simply use the approximation

$$E\left(\alpha_j(X)X_i\right) \;\approx\; \alpha_j(\mu)\mu_i + \tfrac{1}{2!}\sum_{i=1}^{n}\sum_{k=1}^{n} E\left((X_i - \mu_i)(X_k - \mu_k)\right)\tfrac{\partial^2}{\partial x_i \partial x_k}f_j(\mu).$$

This approximation is then inserted into Eq. (8) and the result replaces the term $\tfrac{d}{dt}E\left(X_i X_k\right)$ in Eq. (7). Finally, we can integrate the time evolution of the means and that of the covariances and variances.

EXAMPLE 3. *To illustrate the method we consider again the simple dimerization reaction system of Example 1. Assuming that all central moments of order three and higher are equal to zero, we get the following equations for the means, variances and*

the covariance of the species

$$\frac{d}{dt}\mu_1 = -c_1\mu_1(\mu_1 - 1) - c_1 C_{1,2} + 2c_2\mu_2$$

$$\frac{d}{dt}\mu_2 = \frac{1}{2}c_1\mu_1(\mu_1 - 1) + \frac{1}{2}c_1 C_{1,2} - c_2\mu_2$$

$$\frac{d}{dt}C_{1,1} = -2c_1\mu_1^3 + 4c_1\mu_1^2 - 2c_1\mu_1 + 4c_2\mu_2 + 4c_2\mu_1\mu_2$$

$$\frac{d}{dt}C_{1,2} = -\frac{3}{2}c_1 C_{1,1} + \mu_1\left(-c_1(\mu_1 - 1) - \frac{1}{2}c_1\mu_1 C_{1,1} + c_2\mu_1^2\right)$$
$$\quad +\mu_2\left(-2c_2 - c_2\mu_1 + c_1 C_{1,1}\right)$$

$$\frac{d}{dt}C_{2,2} = \frac{3}{2}c_1 C_{1,1} + \frac{1}{2}c_1\mu_1(\mu_1 - 1) + \mu_2(c_2 - c_1 C_{1,1})$$

where we denote the expectations of species P (P_2) by μ_1 (μ_2), variances are given by $C_{1,1}$, $C_{2,2}$ and the covariance between P and P_2 is $C_{1,2}$. In the equations we omit t to improve readability.

In Section 5 we study the accuracy of the above example (cf. Table II) and find that the approximation provided by moment closure method is very accurate even if only the means and covariances are considered. In general, however, experimental results show that the approximation tends to become worse if systems that exhibit complex behavior such as multistability or oscillations. Increasing the number of moments typically improves the accuracy [Ale et al. 2013] but sometimes the resulting equations may become very stiff [Engblom 2006].

Grima has investigated the accuracy of the approximation for $n = 2$ and $n = 3$ by a comparison with the system size expansion of the master equation [Grima 2012]. He found that for monostable systems with large volumes the approximation of the means $\mu(t)$ have a relative error that scale as Ω^{-n} while the relative errors of the variances and covariances scale as $\Omega^{-(n-1)}$, $n \in \{2, 3\}$. For small volumes or systems with multiple modes, however, only experimental evaluations of the accuracy are available [Ale et al. 2013; Engblom 2006], where the approximated moments are compared to statistical estimates based on Monte Carlo simulations of the process. In Section 5 we focus on experimental results for the reconstructed probability distribution. However, we also compare the moments approximated using the technique described above to the moments obtained by the direct numerical simulation. Note that for the reconstructed probability distributions of the process we have two sources of error: the approximation error of the moment closure and the error associated with the maximum entropy reconstruction as explained below. In our experimental results we therefore apply the reconstruction to both moments obtained from the moment equations as well as the more accurate approximation obtained from a direct numerical simulation. The latter, however, is only possible for systems where the average molecule numbers remain small since otherwise too many states have to be considered during the integration.

4. MAXIMUM ENTROPY RECONSTRUCTION

The moment closure is usually used to approximate the moments of a stochastic dynamical system over time. The numerical integration of the correspondent ODE system is usually faster than a direct integration of the probability distribution or an estimation of the moments based on Monte-Carlo simulations of the system. However, if one is interested in certain events and only the moments of the distribution are known, the corresponding probabilities are not directly accessible and have to be reconstructed based on the moments. Here, we shortly review standard approaches to reconstruct one-dimensional marginal probability distributions $\pi_i(x_i, t) = P(X_i(t) = x_i)$ of a Markov chain that describes the dynamics of chemical reactions network. The task of approximating multi-dimensional distributions follows the same line however for our case these techniques revealed to be not effective due to numerical difficul-

ties in the optimization procedure. Thus, we have given (an approximation of) the moments of the i-th population and obviously, the corresponding distribution is in general not uniquely determined for a finite set of moments. In order to select one distribution from this set, we apply the maximum entropy principle. In this way we minimize the amount of prior information about the distribution and avoid any other latent assumption about the distribution. Taking its roots in statistical mechanics and thermodynamics [Jaynes 1957], the maximum entropy approach was successfully applied to solve moment problems in the field of climate prediction [Abramov et al. 2005; Kleeman 2002; Roulston and Smith 2002], econometrics [Wu 2003], performance analysis [Tari et al. 2005; Guiasu 1986] the and many others.

4.1. Maximum Entropy Approach

The maximum entropy principle says that among the set of allowed discrete probability distributions $\mathcal{G}$ we choose the probability distribution q that maximizes the entropy $H(g)$ over all distributions $g \in \mathcal{G}$, i.e.,

$$q = \arg\max_{g \in \mathcal{G}} H(g) = \arg\max_{g \in \mathcal{G}} \left(- \sum_x g(x) \ln g(x)\right). \quad (10)$$

where x ranges over all possible states of the discrete state space. Note that we assume that all distributions are defined on the same state space. In our case the set $\mathcal{G}$ consists of all discrete probability distributions that satisfy the moment constraints. Given a sequence of M non-central moments

$$E\left(X^k\right) = \mu_k, k = 0, 1, \ldots, M,$$

the following constraints are considered

$$\sum_x x^k g(x) = \mu_k, k = 0, 1, \ldots, M. \quad (11)$$

Here, we choose g to be a non-negative function and add the constraint $\mu_0 = 1$ in order to ensure that g is a distribution. The above problem is a nonlinear constrained optimization problem, which is usually addressed by the method of Lagrange. Consider the Lagrangian functional

$$\mathcal{L}(g, \lambda) = H(g) - \sum_{k=0}^{M} \lambda_k \left(\sum_x x^k g(x) - \mu_k\right),$$

where $\lambda = (\lambda_0, \ldots, \lambda_M)$ are the corresponding Lagrangian multipliers. It is possible to show that maximizing the unconstraint Lagrangian $\mathcal{L}$ gives a solution to the constrained maximum entropy problem The variation of the functional $\mathcal{L}$ according to the unknown distribution provides the general form of $g(x)$

$$\frac{\partial \mathcal{L}}{\partial g(x)} = 0 \implies g(x) = \exp\left(-1 - \sum_{k=0}^{M} \lambda_k x^k\right) = \frac{1}{Z(x)} \exp\left(-\sum_{k=1}^{M} \lambda_k x^k\right),$$

where

$$Z(x) = e^{1+\lambda_0} = \sum_x \exp\left(-\sum_{k=1}^{M} \lambda_k x^k\right)$$

is a normalization constant. In the dual approach we insert the above equation for $g(x)$ into the Lagrangian thus we can transform the problem into an unconstrained convex minimization problem of the dual function w.r.t to the dual variable λ

$$\Psi(\lambda) = \ln Z(x) + \sum_{k=1}^{M} \lambda_k \mu_k,$$

According to the Kuhn-Tucker theorem, the solution $\lambda^* = \arg\min \Psi(\lambda)$ of the minimization problem for the dual function equals the solution q of the original constrained optimization problem (10).

4.2. Maximum Entropy Numerical Approximation

It is possible to solve the constrained maximization problem (10) for $m \leq 2$ analytically. For $m > 2$ numerical methods have to be applied to incorporate the knowledge of moments of order three and more. Possible numerical solution techniques include the Newton minimization procedure [Mead and Papanicolaou 1984], the iterative minimization [Bandyopadhyay et al. 2005] and the application of the Broyden-Fletcher-Goldfarb-Shanno (BFGS) procedure [Byrd et al. 1995]. For our experimental results, we used the algorithm proposed by Abramov [Abramov 2010] and the corresponding software [1]. It can be used to reconstruct distributions with up to 4 dimensions. Due to the difficulties in the numerical optimization procedure here we restrict ourselves to the the reconstruction of one-dimensional marginal distributions $q_i(\cdot)$ that approximate $\pi_i(\cdot, t)$. The essential idea of the algorithm is preconditioning of the original problem to overcome numerical difficulties. This standardization is conducted through a sequence of linear transformations of coordinates in phase space. They include shifting of the moments, rescaling its values to shorten the difference between orders of magnitudes and representing the optimization problem in the generalized orthogonal polynomial basis to lower the sensitivity of the Lagrange multipliers to high values of monomials x^i. After this sequence of preconditioning steps is completed, the optimization BFGS procedure is used to obtain the Lagrangian multipliers λ^*. Solving the ODE system for moments we obtain an approximation of the moment values and thus the distribution with such moments might not exist. This is not a problem in our case since both the number of points in the Gauss-Hermite quadrature formula used in integral computation and the tolerance for optimization procedure are controllable in the implementation we use, so that the optima (if it exists) can be found even using the approximated values. Theoretical conditions for existence of the solution for moment problem are elaborated in detail in [Tari et al. 2005; Stoyanov 2000; Lin 1997]. The similar analysis for the multivariate case is provided in [Kleiber and Stoyanov 2013].

Abramov focuses on continuous state spaces and reconstructs densities instead of discrete probabilities. However, it turns out that the computed densities can be easily transformed into discrete distributions (cf. Section 5). The probability distributions $\pi_i(\cdot, t)$ we are interested in are discrete and in order to approximate the discrete probability $P(X_i = x_i)$ for a molecule count x_i of the i-th species we integrate the reconstructed density q_i and set

$$\tilde{\pi}_i(x_i, t) = \begin{cases} \int\limits_{x_i - \frac{1}{2}}^{x_i + \frac{1}{2}} q_i(x)\,\mathrm{dx}, & x_i > 0 \\ 2 \cdot \int\limits_{0}^{x_i + \frac{1}{2}} q_i(x)\,\mathrm{dx}, & x_i = 0 \end{cases} \tag{12}$$

Additionally we have to truncate the support $\mathbb{R}$ of q_i to $\mathbb{R}^+$ such that $q_i(x) = 0$ for all $x \in (-\infty, 0)$. This can be done by adjusting the normalization constant $Z(x)$ accordingly. The two of three models we are considering have the unbounded state space which does not allow to simplify the process of moment computation in the maximum entropy optimization procedure thus they are approximated by Gauss-Hermite quadrature formula.

---

[1]The software is available at http://homepages.math.uic.edu/~abramov/

5. NUMERICAL RESULTS

In this section we show experimental results of the maximum entropy approach when it is applied to the moments of a reaction network. To estimate the quality of the probability distribution reconstruction, we compare the obtained distributions to those obtained via a direct numerical simulation. Thus, we consider only systems which are small and where a direct numerical simulation is possible. Clearly, for more complex systems with high population sizes a direct numerical simulation is not feasible while the running time of the moment closure approximation is independent of the population sizes.

In order to distinguish errors that are introduced by the moment closure approximation from errors introduced by the reconstruction, we also compare the obtained moments with those computed based on the distributions obtained via direct numerical simulation. Moreover, we applied the maximum entropy approach to the more accurate approximation of the moments obtained via direct numerical simulation. It is important to note that in all cases the maximum entropy optimization only takes less than one second. We therefore only list the running time of the moment closure method.

5.1. Simple Dimerization system

We first consider Example 1 and investigate the numerical accuracy of the moment equations for this example. The moment closure approximation only takes less than one second for this example and Table II compares the moments approximated with the moment closure with the moments obtained from the direct numerical simulation (as described in Section 2.3).

The first column refers to the highest order of the moments that was considered during the computation, i.e., all central moments of higher order are approximated with zero. In addition we list the relative errors of the means (error ord. 1) and the moments of higher order k using the error norm

$$\max_i \frac{|\hat{m}_i^{(k)} - m_i^{(k)}|}{m_i^{(k)}}.$$

Here $\hat{m}_i^{(k)}$ and $m_i^{(k)}$ are the values of moments $E(X_i^k)$ computed using the moment closure method and obtained via direct numerical simulation and the maximum is taken over the chemical species. The second column in tables refers to the number of equations that were integrated for the moment closure method. The initial protein numbers are chosen as $P = 301$ and $P_2 = 0$ and we consider the system at time $t = 20$ [Ale et al. 2013]. We find that the moment closure approximation provides very accurate results.

Next, we reconstruct the marginal distributions of the species P and P_2 and compare then with those obtained using the direct numerical simulation (where we chose $\delta = 10^{-15}$ yielding a total approximation error of $\epsilon = 5 \cdot 10^{-15}$, see also Eq. (3)). For instance, to reconstruct the distribution of P we used the sequence of moments $\mu_0, \ldots, \mu_k$, where $\mu_j = E(X_1^j(t))$ and $X_1(t)$ represents the number of molecules of type P at time t.

Table II: Errors of the moment closure approximation for the dimerization network

ord.	# equ.	error ord. 1	error ord. 2	error ord. 3	error ord. 4	error ord. 5
2	5	0.001754	0.003495	-	-	-
3	9	0.001752	0.003492	0.005215	-	-
4	14	0.001743	0.003465	0.005211	0.006907	-
5	20	0.001721	0.003418	0.005183	0.006901	0.008555

(a)   (b)
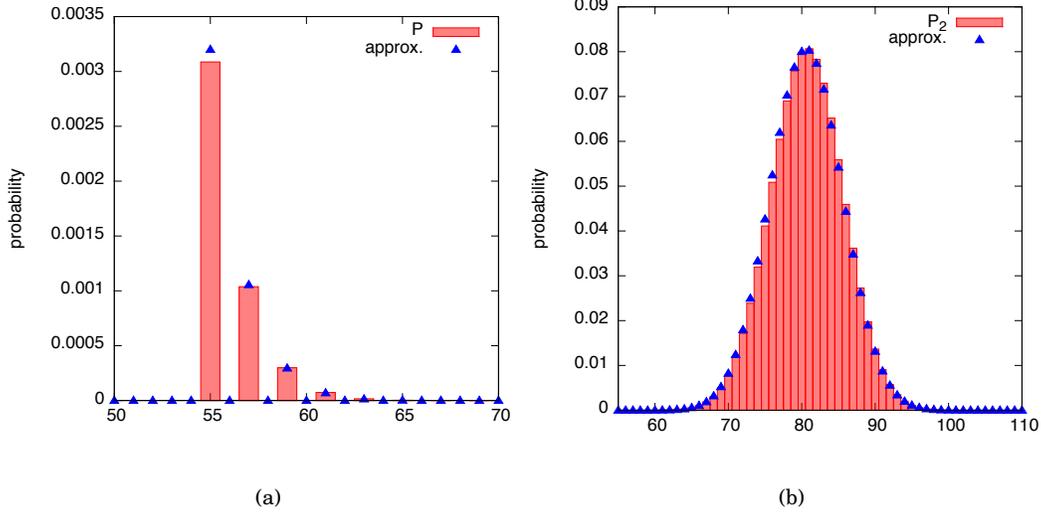
Fig. 2: Maximum entropy reconstruction of marginal probability distributions of the protein counts (a) P and (b) P_2 at time instant $t = 20$ for simple dimerization system.

The values of moments $\mu_0, \ldots, \mu_k$ are approximated by the moment closure method. In Fig. 2 we plot the distribution of P and P_2 where we use red bars for the distribution obtained via direct numerical simulation and blue triangles for the reconstructed distribution (moment closure approximation and maximum entropy reconstruction). For the order of the moments that were considered, we used in for both species the order with which the best approximation was obtained (see below).

In Table III we show how accurate the approximation of individual probabilities $\pi_i(x, t)$ is by calculating the Chebyshev distance

$$||\epsilon_i||_\infty = \max_x |\pi_i(x, t) - \tilde{\pi}_i(x, t)|,$$

where $\pi_i(x, t)$ is the "true" probability of having x molecules of type i at time t (obtained via the accurate direct numerical simulation) and $\tilde{\pi}_i(x, t)$ is the value obtained from the combination of moment closure approximation and maximum entropy reconstruction. The distance is calculated for all non-negative integers x for which $\pi_i(x, t)$ is non-negative, i.e. for species P we only consider every second integer value. In particular,

Table III: Maximum entropy reconstruction results for the dimerization network

ord.	$||\epsilon_P||_\infty$	$||\epsilon_P^*||_\infty$	$||\epsilon_{P_2}||_\infty$	$||\epsilon_{P_2}^*||_\infty$
2	0.001764	0.000623	0.001764	0.000136
3	0.000860	0.000054	0.001782	0.000623
4	0.001683	0.000136	0.001683	0.000053
5	0.001641	0.000132	0.001691	0.000136

we approximate the marginal distribution for P by using a modified form of Eq. 12:

$$\tilde{\pi}_i(x_i, t) = \begin{cases} \int\limits_{x_i-1}^{x_i+1} q_i(x)\, \mathrm{dx}, & x_i > 0 \\ 2 \cdot \int\limits_{0}^{x_i+1} q_i(x)\, \mathrm{dx}, & x_i = 0 \end{cases}$$

In addition, we give the error $||\epsilon_i^*||_\infty$ for the case where the maximum entropy reconstruction was applied to the moments calculated from the results of the direct numerical simulation. We observe that the best maximum entropy method provides the least error when the moments of order up to 3 (for P) and up to 4 (for P_2) are used to reconstruct the marginal distribution. However, the reconstruction is very accurate in all cases and the reason why the Chebyshev distance does not decrease when more moments are considered might be that the properties of the distribution are already well captured by the moments of an order up to three.

5.2. Multi-attractor system

Our second case study is the so-called multi-attractor model [Zhou et al. 2011]. It consists of 23 chemical reactions (listed in Appendix A) and describes the dynamics of three genes and the corresponding proteins. The proteins $PaxProt$, $MAFAProt$ and $DeltaProt$ are able to bind to the promotor regions of the DNA and activate or suppress the production of other proteins. The model is infinite in three dimensions.

Again, we first consider the accuracy of the moment closure approximation (cf. Table IV) in the same way as for the previous example but list the running time in addition (third column). The values or stochastic reaction constants are chosen as $c_p = 5, c_d = 0.1, c_b = 1.0, c_u = 1.0$ and we consider the system at time $t = 10$. As initial conditions we assumed one molecule for all DNA-like species ($\#PaxDna = 1$, $\#MAFADna = 1$, $\#DeltaDna = 1$) and the molecular counts for the remaining species are 0.

We find that the moments obtained via the moment closure approximation are accurately approximated. For instance the average number of $MAFADna$ is approximated as 19.719 while the result of the direct numerical simulation gives 19.544. Note that it takes 20634 seconds to finish the numerical simulation (the size of the truncated state space $|S| = 7736339$) whereas the moment closure approximation takes only 3649 seconds.

Next we consider the reconstruction of the marginal distribution of $PaxProt$, $MAFAProt$ and $DeltaProt$. The results are given in Table V and the best obtained reconstructions are plotted in Figure 3 for all three proteins. We compare the results with the solution of the direct numerical simulation (where we chose $\delta = 10^{-15}$ yielding a total approximation error of $\epsilon = 6 \cdot 10^{-10}$, see also Eq. (3)). We see that the error decreases when more moments are considered. In particular, if all moments up to order 5 are considered, the error is about an order of magnitude lower than the state probabilities around the average molecule count. However, the reconstructed distribution of $DeltaProt$ shows some artifacts, which are due to the bimodal form of the exponential function where the power is given by the polynomial of degree five. We do not observe

Table IV: Moment closure approximation results for the multi-attractor network

ord.	# equ.	time (sec)	error ord. 1	error ord. 2	error ord. 3	error ord. 4	error ord. 5
2	104	2	0.043987	0.077507	-	-	-
3	559	40	0.043987	0.067790	0.104288	-	-
4	2379	443	0.043987	0.058938	0.082293	0.096345	-
5	8567	3649	0.043987	0.037542	0.066227	0.056258	0.110358
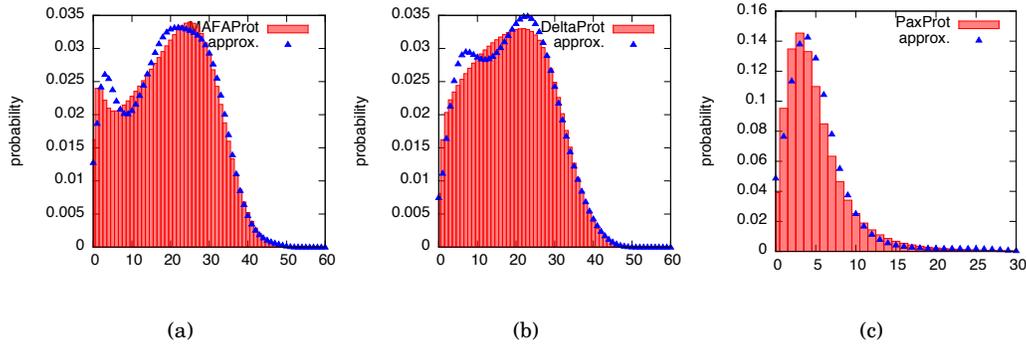
Fig. 3: Maximum entropy reconstruction of marginal probability distributions for multi-attractor system at time instant $t = 10$.

the similar type of artifacts in the reconstructed distribution of $PaxProt$ since there the reconstructed coefficients corresponding to high powers are close to 0.

5.3. Exclusive switch

Finally, we consider the exclusive switch system. We chose reaction rate constants and initial conditions as in Example 2. Again, we first consider the accuracy of the moment closure approximation (cf. Table VI) at time $t = 100$ in the same way as for the previous examples. As also noted by Grima, the error of the moments, that have the highest order considered during the computation, is rather high [Grima 2012]. Thus, in the moment closure approximation we have to consider at least all moment up to order five to accurately estimate the moments up to order four.

Next we compare the marginal distributions of proteins P_1 and P_2 at $t = 60$ (cf. Table VII) and at $t = 100$ (cf. Table VIII) obtained via a direct numerical simulation (choosing $\delta = 10^{-15}$ yielding $\epsilon = 6 \cdot 10^{-11}$ at time $t = 60$ and $\epsilon = 8 \cdot 10^{-11}$ at time $t = 100$) with the distributions obtained from the maximum entropy reconstruction. We see that the qualitative property of the system, the bimodality, is well-described by the moments up to an order of at least four. Thus, it is possible to encode such qualitative properties in the moments. The corresponding plots of the marginal distributions and their reconstructions are given in Figure 4 for $t = 60$ (Figure 5 for $t = 100$). If only the means and covariances are considered, the distribution is not accurately reconstructed, $||\epsilon_{P_1}^*||_\infty$ is of the same order as the maximal state probabilities. As expected the error decreases when moments of higher order are taken into account.

6. CONCLUSIONS

We investigated the accuracy and efficiency of a combination of two methods, the moment closure method and the maximum entropy method, which can be used to analyze

Table V: Maximum entropy reconstruction results for the multi-attractor system

ord.	$\|\epsilon_{\text{MAFAProt}}\|_\infty$	$\|\epsilon_{\text{MAFAProt}}^*\|_\infty$	$\|\epsilon_{\text{DeltaProt}}\|_\infty$	$\|\epsilon_{\text{DeltaProt}}^*\|_\infty$	$\|\epsilon_{\text{PaxProt}}\|_\infty$	$\|\epsilon_{\text{PaxProt}}^*\|_\infty$
2	0.016082	0.012322	0.009978	0.009186	0.053345	0.033673
3	0.012075	0.009372	0.009904	0.009728	0.037701	0.031701
4	0.009030	0.008892	0.009541	0.007568	0.033590	0.027062
5	0.006117	0.005308	0.007053	0.005295	0.030783	0.021304

Table VI: Moment closure approximation results for the exclusive switch

ord.	# equ.	time (sec)	error ord. 1	error ord. 2	error ord. 3	error ord. 4	error ord. 5
2	20	< 1	0.004555	0.194240	-	-	-
3	55	< 1	0.004555	0.026281	0.060490	-	-
4	125	2	0.004555	0.020493	0.028242	0.136965	-
5	251	6	0.004555	0.017774	0.027933	0.026724	0.015461

(a)   (b)
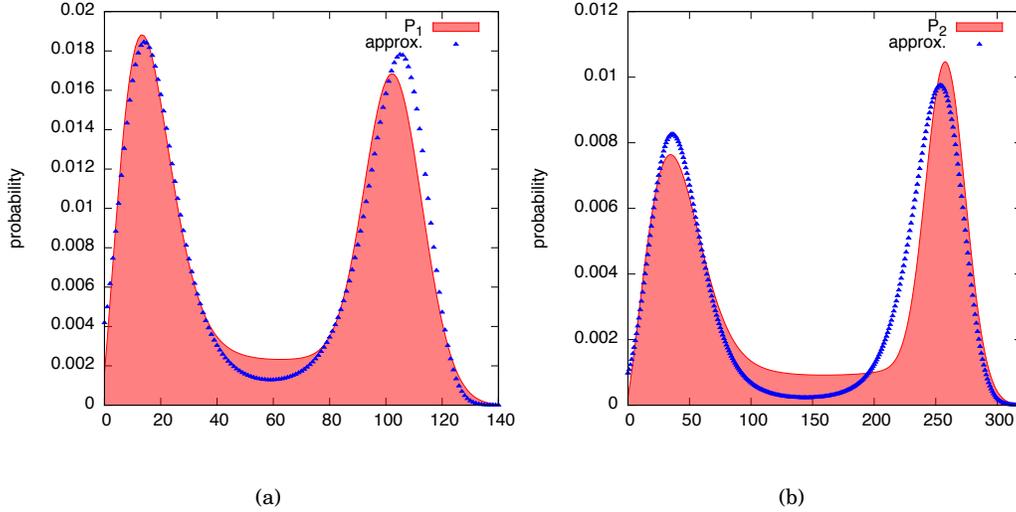
Fig. 4: Maximum entropy reconstruction of marginal probability distributions of the protein counts (a) P_1 and (b) P_2 at time instant $t = 60$ for exclusive switch system.

stochastic models of biochemical reaction networks. With the chemical master equation as a starting point we described how the moments of the corresponding probability distributions can be integrated efficiently over time and how a distribution can be reconstructed based on the moments. Our experimental results show that the proposed combination of methods has many advantages. It is a fast and surprisingly accurate way of obtaining the distribution of the system at specific points in time and therefore well suited for computationally expensive tasks such as the approximation of likelihoods or event probabilities.

As future work, we plan to extend the reconstruction procedure in several ways. First, we want to consider moments of higher order than five. Since in this case the concrete values become very large it might be advantageous to consider central moments instead which implies that the reconstruction procedure has to be adapted. Al-

Table VII: Maximum entropy reconstruction results for the exclusive switch at time $t = 60$

ord.	$\|\epsilon_{P_1}\|_\infty$	$\|\epsilon^*_{P_1}\|_\infty$	$\|\epsilon_{P_2}\|_\infty$	$\|\epsilon^*_{P_2}\|_\infty$
2	0.013655	0.013630	0.008134	0.0081149
3	0.013409	0.013206	0.008074	0.007808
4	0.004844	0.003084	0.002154	0.002117
5	0.003837	0.002541	0.001878	0.001757

(a)   (b)
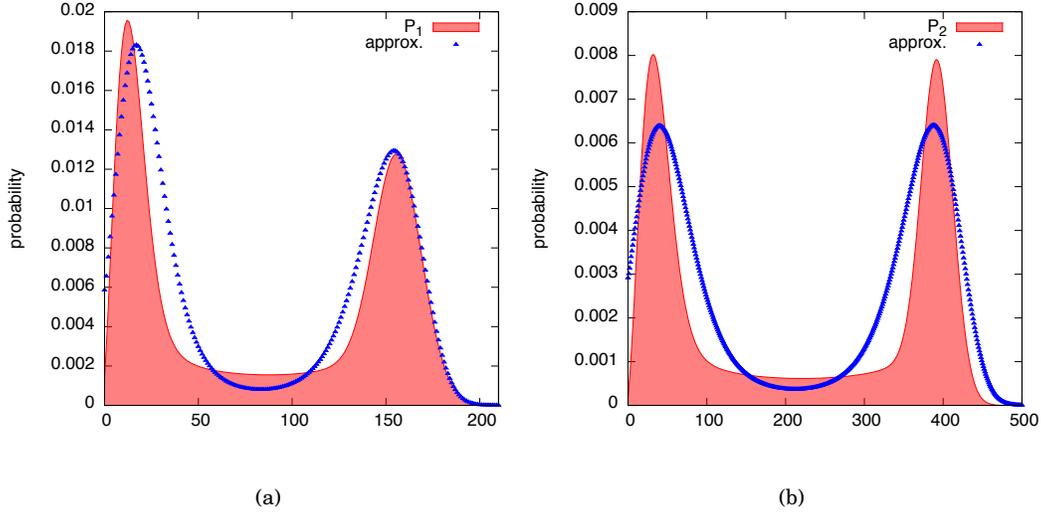
Fig. 5: Maximum entropy reconstruction of marginal probability distributions of the protein counts (a) P_1 and (b) P_2 at time instant $t = 100$ for exclusive switch system.

ternatively, we might (instead of algebraic moments) consider other functions of the random variables such as exponential functions [Mnatsakanov and Sarkisian 2013], Fup functions [Gotovac and Gotovac 2009], and Chebyshev polynomials [Bandyopadhyay et al. 2005]. Another possible extension could address the problem of truncating the support of the distribution such that the reconstruction is applied to a finite support. We expect that in this case the reconstruction will become more accurate since we will not have to rely on the Gauss-Hermite quadrature formula. For instance, the theory of Christoffel functions [Gavriliadis and Athanassoulis 2012] could be used to determine the region where the main part of the probability mass is located.

Finally, we want to improve the approximation for species that are present in very small quantities, since for those species a direct representation of the probabilities is more appropriate than a moment representation. Therefore we plan to consider the conditional moments approach [Hasenauer et al. 2013], where we only integrate the moments of species having large molecular counts but keep the discrete probabilities for the species with small populations.

Table VIII: Maximum entropy reconstruction results for the exclusive switch at time $t = 100$

ord.	$\|\epsilon_{P_1}\|_\infty$	$\|\epsilon^*_{P_1}\|_\infty$	$\|\epsilon_{P_2}\|_\infty$	$\|\epsilon^*_{P_2}\|_\infty$
2	0.016287	0.016281	0.006732	0.006563
3	0.016270	0.016253	0.006746	0.005158
4	0.007783	0.007277	0.003983	0.003301
5	0.007527	0.007016	0.002733	0.002455

REFERENCES

R. Abramov. 2010. The multidimensional maximum entropy moment problem: a review of numerical methods. Communications in Mathematical Sciences 8, 2 (2010), 377–392.

R. Abramov, A. Majda, and R. Kleeman. 2005. Information theory and predictability for low-frequency variability. Journal of the atmospheric sciences 62, 1 (2005), 65–87.

A. Ale, P. Kirk, and M. P. H. Stumpf. 2013. A general moment expansion method for stochastic kinetic models. The Journal of Chemical Physics 138, 17 (2013).

G. Amos, J. George, and K. Larry. 1996. A maximum entropy approach to estimation and inference in dynamic models or Counting fish in the sea using maximum entropy. Journal of Economic Dynamics and Control 20, 4 (1996), 559 – 582.

A. Andreychenko, P. Crouzen, and V. Wolf. 2011. On-the-fly Uniformization of Time-Inhomogeneous Infinite Markov Population Models. In Proceedings of the 9th International Workshop on Quantitative Aspects of Programming Languages (QAPL'11), Vol. 57. Elsevier Science, 1.

A. Andreychenko, L. Mikeev, D. Spieler, and V. Wolf. 2012. Approximate maximum likelihood estimation for stochastic chemical kinetics. EURASIP Journal on Bioinformatics and Systems Biology 9 (2012).

K. Bandyopadhyay, A. K. Bhattacharya, P. Biswas, and D. A. Drabold. 2005. Maximum entropy and the problem of moments: A stable algorithm. Physical Review E 71, 5 (2005), 057701/1–057701/4.

R. H. Byrd, P. Lu, J. Nocedal, and C. Zhu. 1995. A limited memory algorithm for bound constrained optimization. SIAM Journal on Scientific Computing 16, 5 (1995), 1190–1208.

D. E. Chauveau, A. C. M. Vanrooij, and F. H. Ruymgaart. 1994. Regularized Inversion of Noisy Laplace Transforms. Advances in Applied Mathematics 15, 2 (1994), 186 – 201.

S. X. Chen. 2000. Probability Density Function Estimation Using Gamma Kernels. Annals of the Institute of Statistical Mathematics 52, 3 (2000), 471–480.

T. Dayar, H. Hermanns, D. Spieler, and V. Wolf. 2011. Bounding the Equilibrium Distribution of Markov Population Models. Numerical Linear Algebra with Applications 18 (2011), 931–946. Issue 6.

M. B. Elowitz, M. J. Levine, E. D. Siggia, and P. S. Swain. 2002. Stochastic Gene Expression in a Single Cell. Science 297 (2002), 1183–1186.

S. Engblom. 2006. Computing the moments of high dimensional solutions of the master equation. Appl. Math. Comput 180 (2006). Issue 2.

N. Fedoroff and W. Fontana. 2002. Small Numbers of Big Molecules. Science 297 (2002), 1129–1131.

P.N. Gavriliadis. 2008. Moment information for probability distributions, without solving the moment problem. I: Where is the mode? Communications in Statistics - Theory and Methods 37, 5 (2008), 671–681.

P. N. Gavriliadis and G. A. Athanassoulis. 2012. The truncated Stieltjes moment problem solved by using kernel density functions. *J. Comput. Appl. Math.* 236, 17 (2012), 4193–4213.

D. T. Gillespie. 1977. Exact stochastic simulation of coupled chemical reactions. Journal of Physical Chemistry 71, 25 (1977), 2340–2361.

H. Gotovac and B. Gotovac. 2009. Maximum entropy algorithm with inexact upper entropy bound based on Fup basis functions with compact support. *J. Comput. Phys.* 228, 24 (2009), 9079–9091.

R. Grima. 2012. A study of the accuracy of moment-closure approximations for stochastic chemical kinetics. The Journal of Chemical Physics 136, 15 (2012), 4105.

S. Guiasu. 1986. Maximum entropy condition in queueing theory. Journal of the Operational Research Society (1986), 293–301.

J. Hasenauer, V. Wolf, A. Kazeroonian, and F.J. Theis. 2013. Method of conditional moments (MCM) for the Chemical Master Equation. Journal of Mathematical Biology (2013), 1–49.

T. Jahnke and W. Huisinga. 2007. Solving the chemical master equation for monomolecular reaction systems analytically. Journal of Mathematical Biology 54, 1 (2007), 1–26.

E. T. Jaynes. 1957. Information Theory and Statistical Mechanics. Phys. Rev. 106 (1957), 620–630.

R. Kaas and M. J. Goovaerts. 1986. Best bounds for positive distributions with fixed moments. Insurance: Mathematics and Economics 5, 1 (1986), 87 – 92.

R. Kleeman. 2002. Measuring dynamical prediction utility using relative entropy. Journal of the atmospheric sciences 59, 13 (2002), 2057–2072.

C. Kleiber and J. Stoyanov. 2013. Multivariate distributions and the moment problem. Journal of Multivariate Analysis 113 (2013), 7–18.

G. D. Lin. 1997. On the moment problems. Statistics and Probability Letters 35, 1 (1997), 85–90.

A. Loinger, A. Lipshtat, N. Q. Balaban, and O. Biham. 2007. Stochastic Simulations of Genetic Switch Systems. Physical Review E 75 (2007), 021904.

M. Mateescu, V. Wolf, F. Didier, and T. A. Henzinger. 2010a. Fast Adaptive Uniformisation of the Chemical Master Equation. IET Systems Biology 4, 6 (2010), 441–452.

M. Mateescu, V. Wolf, F. Didier, and T. A. Henzinger. 2010b. Fast Adaptive Uniformisation of the Chemical Master Equation. IET Systems Biology Journal 4, 6 (2010).

H. H. McAdams and A. Arkin. 1999. It's a noisy business! Trends in Genetics 15, 2 (1999), 65–69.

D. A. McQuarrie. 1967. Stochastic approach to chemical kinetics. Journal of Applied Probability 4 (1967), 413–478.

L. R. Mead and N. Papanicolaou. 1984. Maximum entropy in the problem of moments. *J. Math. Phys.* 25 (1984), 2404.

L. Mikeev, S. Werner, and V. Wolf. 2011. Efficient Calculation of Rare Event Probabilities in Markovian Queueing Networks. In Proceedings of the 5th International ICST Conference on Performance Evaluation Methodologies and Tools (VALUETOOLS '11). 186–196.

R. M. Mnatsakanov and A. S. Hakobyan. 2009. Recovery of Distributions via Moments. In Institute of Mathematical Statistics Lecture Notes - Monograph Series. 252–265.

R. M. Mnatsakanov and K. Sarkisian. 2013. A note on recovering the distributions from exponential moments. *Appl. Math. Comput.* 219, 16 (2013), 8730–8737.

B. Munsky and M. Khammash. 2006. The Finite State Projection Algorithm for the Solution of the Chemical Master Equation. J. Chem. Phys. 124 (2006), 044144.

M. S. Roulston and L. A. Smith. 2002. Evaluating probabilistic forecasts using information theory. Monthly Weather Review 130, 6 (2002), 1653–1660.

J. Ruess, A. Milias, and J. Lygeros. 2013. Designing experiments to understand the variability in biochemical reaction networks. Journal of the Royal Society Interface 10, 88 (2013), 20130588.

P. Smadbeck and Y. N. Kaznessis. 2013. A closure scheme for chemical master equations. Proceedings of the National Academy of Sciences 110, 35 (2013), 14261–14265.

J. Stoyanov. 2000. Krein Condition in Probabilistic Moment Problems. Bernoulli 6, 5 (2000), pp. 939–949.

A. Tari, M. Telek, and P. Buchholz. 2005. A Unified Approach to the Moments Based Distribution Estimation Unbounded Support. In Formal Techniques for Computer Systems and Business Processes. Number 3670 in Lecture Notes in Computer Science. 79–93.

M. Thattai and van Oudenaarden A. 2001. Intrinsic Noise in Gene Regulatory Networks. PNAS, USA 98, 15 (2001), 8614–8619.

X. Wu. 2003. Calculation of maximum entropy densities with application to income distribution. 115, 2 (2003), 347–354.

X. Wu. 2009. A Weighted Generalized Maximum Entropy Estimator with a Data-driven Weight. Entropy 11, 4 (2009), 917–930.

J. X. Zhou, L. Brusch, and S. Huang. 2011. Predicting pancreas cell fate decisions and reprogramming with a hierarchical multi-attractor model. PloS one 6, 3 (2011), 14752.

A. REACTIONS OF THE MULTI-ATTRACTOR MODEL

The multi-attractor model involves the three species *MAFAProt*, *DeltaProt*, and *PaxProt* that represent the proteins of the three genes and it involves ten species that represent the state of the genes: *PaxDna*, *MAFADna*, *DeltaDna*, *PaxDnaDeltaProt*, *MAFADnaPaxProt*, *MAFADnaMAFAProt*, *MAFADnaDeltaProt*, *DeltaDnaPaxProt*, *DeltaDnaMAFAProt*, *DeltaDnaDeltaProt*. The chemical reactions are as follows:

$$
\begin{aligned}
PaxDna &\xrightarrow{c_p} PaxDna + PaxProt \\
PaxProt &\xrightarrow{c_d} \emptyset \\
PaxDna + DeltaProt &\xrightarrow{c_b} PaxDnaDeltaProt \\
PaxDnaDeltaProt &\xrightarrow{c_u} PaxDna + DeltaProt \\
MAFADna &\xrightarrow{c_p} MAFADna + MAFAProt \\
MAFAProt &\xrightarrow{c_d} \emptyset \\
MAFADna + PaxProt &\xrightarrow{c_b} MAFADnaPaxProt \\
MAFADnaPaxProt &\xrightarrow{c_u} MAFADna + PaxProt \\
MAFADnaPaxProt &\xrightarrow{c_p} MAFADnaPaxProt + MAFAProt \\
MAFADna + MAFAProt &\xrightarrow{c_b} MAFADnaMAFAProt \\
MAFADnaMAFAProt &\xrightarrow{c_u} MAFADna + MAFAProt \\
MAFADnaMAFAProt &\xrightarrow{c_p} MAFADnaMAFAProt + MAFAProt \\
MAFADna + DeltaProt &\xrightarrow{c_b} MAFADnaDeltaProt \\
MAFADnaDeltaProt &\xrightarrow{c_u} MAFADna + DeltaProt \\
DeltaDna &\xrightarrow{c_p} DeltaDna + DeltaProt \\
DeltaProt &\xrightarrow{c_d} \emptyset \\
DeltaDna + PaxProt &\xrightarrow{c_b} DeltaDnaPaxProt \\
DeltaDnaPaxProt &\xrightarrow{c_u} DeltaDna + PaxProt \\
DeltaDnaPaxProt &\xrightarrow{c_p} DeltaDnaPaxProt + DeltaProt \\
DeltaDna + MAFAProt &\xrightarrow{c_b} DeltaDnaMAFAProt \\
DeltaDnaMAFAProt &\xrightarrow{c_u} DeltaDna + MAFAProt \\
DeltaDna + DeltaProt &\xrightarrow{c_b} DeltaDnaDeltaProt \\
DeltaDnaDeltaProt &\xrightarrow{c_u} DeltaDna + DeltaProt \\
DeltaDnaDeltaProt &\xrightarrow{c_p} DeltaDnaDeltaProt + DeltaProt
\end{aligned}
\tag{13}
$$